Numerical Solution for Min-Max Shape Optimization Problems*
(Minimum Design of Maximum Stress and Displacement)

Masatoshi SHIMODA**, Hideyuki AZEGAMI*** and Toshiaki SAKURAI**

This paper presents a numerical shape optimization method for continua that minimizes some maximum local measure such as stress or displacement. A method of solving such min-max problems subject to a volume constraint is proposed. This method uses the Kreisselmeier-Steinhauser function to transpose local functionals to global integral functionals so as to avoid non-differentiability. With this function, a multiple loading problem is recast as a single loading problem. The shape gradient functions used in the proposed traction method are derived theoretically using Lagrange multipliers and the material derivative method. Using the traction method, the optimum domain variation that reduces the objective functional is numerically and iteratively determined while maintaining boundary smoothness. Calculated results for two- and three-dimensional problems are presented to show the effectiveness and practical utility of the proposed method for min-max shape design problems.

Key Words: Optimum Design, Finite Element Method, Shape Optimization, Min-Max Problem, Kreisselmeier-Steinhauser Function, Traction Method, Material Derivative Method, Adjoint Method, Multiple Loading.

1. Introduction

In structural design, it is often necessary to determine the optimal shape that maximizes strength for a given material. This can be accomplished by minimizing the maximum value of some local measure (e.g., von Mises stress) with respect to the strength criterion of the material to be used. Another design requirement often encountered is the need to maximize rigidity so as to minimize displacement in cases where the latter is the evaluation measure and its maximum value is an index of the former. These represent examples of what are called min-max problems the objective of which is to minimize the maximum value of a local state variable or its function (both of which will be referred to here as a local measure). This paper concerns min-max shape optimization problems in which the local measure is von Mises stress or the displacement norm, and the boundary shape is treated as the design variable.

In general, such min-max problems contain the following latent difficulties. One difficulty is the occurrence of non-differentiability in relation to domain variation because of the local property of the maximum measure, i.e., the objective functional. This problem can occur because the functions in the functional are not smooth or because the maximum value may jump to another location as a result of domain variation. Moreover, when using the adjoint variable method to find the sensitivity, the issue of singularity can occur because the virtual load becomes a delta function. As a way to avoid these problems, Banichuk[1] proposed a method whereby the l_p norm is used to transpose a local functional into an integral functional. In addition, Taylor and Bendsøe[2] used a method referred to as the bound formulation or β method to change the value of the maximum stress constraint to the objective functional. Trompette et al.[3] and Kristensen et al.[4] have also applied similar approaches to shape optimization problems involving

* Received 3rd July, 1997. Japanese original: Trans. Jpn. Soc. Mech. Eng., Vol. 63, No. 607, A (1997), p. 610-617 (Received 22nd July, 1996)
** Mitsubishi Motors Corporation, 1 Nakashinkiri, Hashime-cho, Okazaki-city, Aichi-pref. 444, Japan
*** Toyohashi University of Technology, 1-1 Hibarigaoka, Tempaku-cho, Toyohashi-city, Aichi-pref. 441, Japan

fillets or holes. By transforming the problem to a solvable formulation, min-max problems can be treated as ordinary minimization problems.

The authors, on the other hand, have applied the traction method[5] to derive solutions to boundary shape optimization problems, including stress square error minimization problems[6] and homologous deformation problems[7]. Grounded in the variational method and optimal control, the traction method has been proposed as a procedure for solving shape optimization problems. It provides a numerical procedure for determining the amount of domain variation that minimizes the objective functional, using the gradient method in a Hilbert space. By deriving the shape sensitivity function (shape gradient function) and treating the design variable (boundary shape) as a function, it is possible to design boundary shapes having many degrees of freedom, without limiting the latitude of design freedom.

This paper describes the application of the traction method to obtain solutions to boundary shape optimization problems in which a maximum local measure is the objective functional. The problems treated here are min-max stress problems and min-max displacement problems involving a multiobjective structure subject to multiple loading. Few studies of such problems are found in the literature. The Kreisselmeier-Steinhauser (KS) function[8], proposed for use in solving optimal control problems, is used to transform the local measure (von Mises stress or the displacement norm) to an integral functional and to scalarize the vector objective functional. The proposed method makes it possible to design shapes that minimize the maximum stress or maximum displacement.

First, the problems will be formulated, and the shape gradient function will be derived using the Lagrange multiplier method or the adjoint variable method and the material derivative method. Then, procedures for analyzing the shape gradient function, including the adjoint variable, and domain variation based on the traction method will be presented. Finally, the computed results for typical two- and three-dimensional problems will be presented to demonstrate the effectiveness of the proposed method for solving min-max local measure problems in which the design boundary is taken as the design variable and the objective is to minimize the maximum stress or displacement.

2. Min-Max Local Measure Problems

Consider a minimization problem of a local measure subject to multiple loading under a condition of a volume constraint. The local measures considered here are von Mises stress in a strength maximization problem and the displacement norm in a rigidity maximization problem. The shape gradient function of each problem will be derived theoretically.

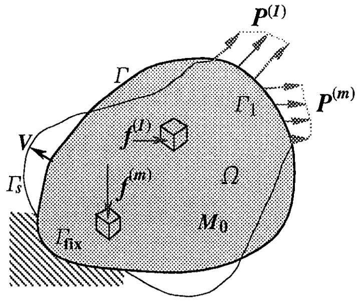

Fig. 1 Domain variation of continuum

2.1 Problem formulation

As shown in Fig. 1, we will assume that a linear elastic continuum having an initial domain of Ω and boundary of $\Gamma \equiv \partial\Omega$ undergoes variation $\boldsymbol{V}$ such that its domain and boundary become Ω_s and $\Gamma_s \equiv \partial\Omega_s$. The notation Γ_{design} denotes the variable design boundary, and multiple body forces $\boldsymbol{f}^{(m)}$ and surface tractions $\boldsymbol{P}^{(m)}(m=1, 2, \cdots, N)$ are assumed to act on Ω_s and Γ_1, respectively. It is also assumed that N load cases act independently. The notation s indicates the iteration history of domain variation.

It is necessary to express the objective functional in an integral form in order to avoid the above-mentioned problems of non-differentiability and singularity due to the local property of the maximum measure. This representation is also needed to formulate the problem as a distributed parameter optimization problem so as to allow application of the traction method. Additionally, this optimization problem subject to multiple loading will be treated as a vector optimization problem. To allow easy treatment of the problem, it must be scalarized to a single objective optimization problem. The KS function is introduced here to resolve these issues.

2.2 *KS* function

The KS function is defined as

$$KS_1(\phi^{(m)}(x)) = \frac{1}{\rho}\ln\sum_{m=1}^{N}\exp(\phi^{(m)}(x)\cdot\rho) \qquad (1)$$

A sufficiently smooth function enveloping the maximum value of N number of measure functions $\phi^{(m)}(x)$ is obtained with this expression when ρ is sufficiently large, as shown in Fig. 2. In actuality, a value of ρ in a range of 5 to 200 is used[9]. By expressing a single measure function $\phi(x)$ in an integral form as indicated in Eq. (2), its maximum value can be extracted when ρ is sufficiently large.

$$KS_2(\phi(x)) = \frac{1}{\rho}\ln\int_{\Omega}\exp(\phi(x)\cdot\rho)dx \qquad (2)$$

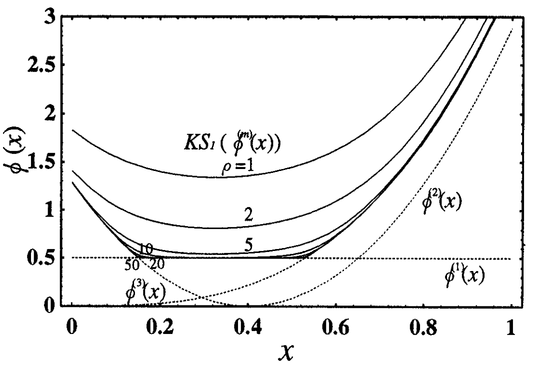

Fig. 2 *KS* function

2. 3 Objective functional

The objective functional of a minimization problem of a maximum measure subject to multiple loading can generally be expressed as

$$\max_{m=1,\cdots,N}\max_{x\in\Omega_S}\left[\frac{\phi^{(m)}(x)}{\phi_a}\right]=\max_{x\in\Omega_S}\max_{m=1,\cdots,N}\left[\frac{\phi^{(m)}(x)}{\phi_a}\right] \quad (3)$$

Since this local functional contains the inherent difficulties noted earlier, we will transpose it to an integral functional of a single solvable objective by combining the *KS* function of Eqs. (1) and (2). This produces the following expression :

$$\frac{1}{\rho}\ln\int_{\Omega_S}\left\{\sum_{m=1}^{N}\exp\left(\frac{\phi^{(m)}(x)}{\phi_a}\cdot\rho\right)\right\}dx \quad (4)$$

where ϕ_a is a normalization constant.

2. 4 Min-max stress problem

When von Mises stress is considered as the local measure, a min-max stress problem can be stated as noted below using Eq. (4), with volume and the state equations of each load case used as constraints.

Given Ω, $\boldsymbol{f}^{(m)}$ in Ω, $\boldsymbol{P}^{(m)}$ on Γ_1, $\boldsymbol{e}$ in Ω, $M_0\in\mathbb{R}_+$ (5)

find Ω_S (or $\boldsymbol{V}$) (6)

$$\text{that minimize } \frac{1}{\rho}\ln\int_{\Omega_S}\left\{\sum_{m=1}^{N}\exp\left(\frac{\sigma_M^{(m)}}{\sigma_a}\cdot\rho\right)\right\}dx \quad (7)$$

subject to $M-M_0\leq 0$ (8)

$$a(\boldsymbol{v}^{(m)},\boldsymbol{w}^{(m)})=l(\boldsymbol{w}^{(m)})$$
$$\text{for all } \boldsymbol{w}^{(m)}\in U, \boldsymbol{v}^{(m)}\in U,\ m=1,\cdots,N \quad (9)$$

where σ_M is the von Mises stress defined by Eq. (10).

$$\sigma_M^2=\frac{1}{2}\{(\sigma_{xx}-\sigma_{yy})^2+(\sigma_{yy}-\sigma_{zz})^2+(\sigma_{zz}-\sigma_{xx})^2+6(\sigma_{xy}^2+\sigma_{yz}^2+\sigma_{xz}^2)\} \quad (10)$$

Additionally, the bilinear form $a(\boldsymbol{v}^{(m)},\boldsymbol{w}^{(m)})$ that gives the variational strain energy with respect to the m-th load case and the linear form $l(\boldsymbol{w}^{(m)})$ that gives the variational potential energy due to external forces are defined by Eqs. (11) and (12). In these equations, $\boldsymbol{v}^{(m)}$ and $\boldsymbol{w}^{(m)}$ indicate the displacement and the variational displacement of load case m, respectively, and U denotes the suitably smooth function space that satisfies the displacement constraint condition. M and M_0 indicate the volume and its constraint value, respectively, and $\mathbb{R}_+$ is a set of positive real numbers.

$$a(\boldsymbol{v}^{(m)},\boldsymbol{w}^{(m)})=\int_{\Omega_S}e_{ijkl}v_{k,l}^{(m)}w_{i,j}^{(m)}d\Omega \quad (11)$$

$$l(\boldsymbol{w}^{(m)})=\int_{\Omega_S}f_i^{(m)}w_i^{(m)}d\Omega+\int_{\Gamma_1}P_i^{(m)}w_i^{(m)}d\Gamma \quad (12)$$

where $\boldsymbol{e}$ (e_{ijkl} in tensor notation) is Hooke's rigidity. The tensor notation employed in this paper uses the Einstein summation convention and a partial differential notation $(\cdot)_{,i}=\partial(\cdot)/\partial x_i$.

Letting $\boldsymbol{w}^{(m)}$ and Λ denote the Lagrange multipliers for the state equations and volume, respectively, the Lagrangian functional L with respect to this problem can be expressed as

$$\begin{aligned}&L(\Omega,\boldsymbol{v}^{(1)},\cdots,\boldsymbol{v}^{(N)},\boldsymbol{w}^{(1)}\cdots,\boldsymbol{w}^{(N)},\Lambda)\\&=\frac{1}{\rho}\ln\int_{\Omega_S}\left\{\sum_{m=1}^{N}\exp\left(\frac{\sigma_M^{(m)}}{\sigma_a}\cdot\rho\right)\right\}dx\\&+\sum_{m=1}^{N}\{l(\boldsymbol{w}^{(m)})-a(\boldsymbol{v}^{(m)},\boldsymbol{w}^{(m)})\}+\Lambda(M-M_0)\end{aligned} \quad (13)$$

For simplicity, it is assumed that the traction boundaries does not change in the normal direction ($n_lV_l=0$ on Γ_1), the material is homogenous and constant ($e'_{ijkl}=\dot{e}_{ijkl}=0$), and the body forces are constant within the domain ($\boldsymbol{f}'=0$). Then, using the speed field $\boldsymbol{V}$ that expresses the domain variation, the derivative $\dot{L}$ in relation to the domain variation of the Lagrangian functional L can be expressed with the material derivative method as

$$\begin{aligned}\dot{L}=&\sum_{m=1}^{N}\{l(\boldsymbol{w}'^{(m)})-a(\boldsymbol{v}^{(m)},\boldsymbol{w}'^{(m)})\}\\&+\sum_{m=1}^{N}\left\{\frac{1}{\sigma_aA}\cdot\int_{\Omega_S}\exp\left(\frac{\sigma_M^{(m)}}{\sigma_a}\cdot\rho\right)\frac{\partial\sigma_M^{(m)}}{\partial\sigma_{ij}}\sigma'_{ij}dx-a(\boldsymbol{v}'^{(m)},\boldsymbol{w}^{(m)})\right\}\\&+\int_{\Gamma_S}\left\{\sum_{m=1}^{N}\left(-e_{ijkl}v_{k,l}^{(m)}w_{i,j}^{(m)}+f_i^{(m)}w_i^{(m)}+\frac{1}{\rho\cdot A}\exp\left(\frac{\sigma_M^{(m)}}{\sigma_a}\cdot\rho\right)\right)+\Lambda\right\}\cdot n_lV_ld\Gamma\\&+\Lambda'(M-M_0),\ \boldsymbol{V}\in\boldsymbol{C}_\Theta\end{aligned} \quad (14)$$

$$A=\int_{\Omega_S}\left\{\sum_{m=1}^{N}\exp\left(\frac{\sigma_M^{(m)}}{\sigma_a}\cdot\rho\right)\right\}dx \quad (15)$$

where $(\cdot)'$ is the shape derivative, $(\dot{\cdot})$ is the material derivative[5], $\boldsymbol{n}$ is an outward unit normal vector and $\boldsymbol{C}_\Theta$ is the suitably smooth function space that satisfies the constraint on domain variation.

The optimality condition with respect to $\boldsymbol{v}$, $\boldsymbol{w}$ and Λ of the Lagrange functional L is expressed as shown below taking into account the stationarity of the inequality constraints.

$$a(\boldsymbol{v}^{(m)},\boldsymbol{w}'^{(m)})=l(\boldsymbol{w}'^{(m)})$$
$$\text{for all } \boldsymbol{w}'^{(m)}\in U,\ m=1,\cdots,N \quad (16)$$

$$\begin{aligned}a(\boldsymbol{v}'^{(m)},\boldsymbol{w}^{(m)})&=\frac{1}{\sigma_aA}\cdot\int_{\Omega_S}\exp\left(\frac{\sigma_M^{(m)}}{\sigma_a}\cdot\rho\right)\cdot\frac{\partial\sigma_M^{(m)}}{\partial\sigma_{ij}}\sigma'_{ij}dx\\&=\frac{1}{\sigma_aA}\cdot\int_{\Omega_S}\exp\left(\frac{\sigma_M^{(m)}}{\sigma_a}\cdot\rho\right)\cdot\frac{\partial\sigma_M^{(m)}}{\partial\sigma_{ij}}\cdot\frac{\partial\sigma_{ij}}{\partial v_k}\cdot v'_kdx\end{aligned}$$

$$\text{for all } \boldsymbol{v}'^{(m)}\in U,\ m=1,\cdots,N \qquad (17)$$

$$\Lambda(M-M_0)=0 \qquad (18)$$

$$M-M_0\leq 0 \qquad (19)$$

$$\Lambda\geq 0 \qquad (20)$$

where Eq.(16) is the governing equation of $\boldsymbol{v}^{(m)}$ and coincides with the state equation, and Eq.(17) is the governing equation of the adjoint variable $\boldsymbol{w}^{(m)}$ which is equivalent to the variational displacement (adjoint equation). Further, Eqs.(18) through (20) are the governing equations of the Lagrangian multiplier Λ with respect to the volume constraint.

Hence, by using $\boldsymbol{v}^{(m)}$, $\boldsymbol{w}^{(m)}$ and Λ which have been determined under the foregoing conditions, the derivative of the Lagrangian functional can be given by

$$\dot{L}=l_G(\boldsymbol{V}) \qquad (21)$$

where the linear form $l_G(\boldsymbol{V})$ of the speed field $\boldsymbol{V}$ is given by the following equation:

$$l_G(\boldsymbol{V})=\int_{\Gamma_s} G_i V_i d\Gamma \qquad (22)$$

$$\boldsymbol{G}=\left\{\sum_{m=1}^{N}\left(-e_{ijkl}v_{k,l}^{(m)}w_{i,j}^{(m)}+f_i^{(m)}w_i^{(m)} +\frac{1}{\rho\cdot A}\cdot\exp\left(\frac{\sigma_M^{(m)}}{\sigma_a}\cdot\rho\right)\right)+\Lambda\right\}\cdot\boldsymbol{n}$$
$$\text{on } \Gamma_{design}\equiv\Gamma\backslash\Gamma_{fix} \qquad (23)$$

It should be noted that $\boldsymbol{G}$ is given on the design boundary and is called the shape gradient function.

2.5 Min-max displacement problem

When the displacement norm $\|v_R\|$ expressed by Eq.(24) is considered as the local measure, the objective functional can be defined as indicated in Eq.(25).

$$\|v_R(x)\|=(v_x^2+v_y^2+v_z^2)^{1/2} \qquad (24)$$

$$\frac{1}{\rho}\ln\int_{\Omega_S}\left\{\sum_{m=1}^{N}\exp\left(\frac{\|v_R^{(m)}(x)\|}{v_a}\cdot\rho\right)\right\}dx \qquad (25)$$

Similar to the strength maximization problem, adjoint Eq.(26) corresponding to Eq.(17) and a shape gradient function (Eq.(28)) corresponding to Eq.(23) can be derived as shown below.

$$a(\boldsymbol{v}'^{(m)},\boldsymbol{w}^{(m)})=\frac{1}{v_a A}\cdot\int_{\Omega_S}\exp\left(\frac{\|v_R^{(m)}\|}{v_a}\cdot\rho\right) \cdot\frac{\partial\|v_R^{(m)}\|}{\partial v_k}v'_k dx$$
$$\text{for all } \boldsymbol{v}'^{(m)}\in U,\ m=1,\cdots,N \qquad (26)$$

$$A=\int_{\Omega_S}\left\{\sum_{m=1}^{N}\exp\left(\frac{\|v_R^{(m)}\|}{v_a}\cdot\rho\right)\right\}dx \qquad (27)$$

$$\boldsymbol{G}=\left\{\sum_{m=1}^{N}\left(-e_{ijkl}v_{k,l}^{(m)}w_{i,j}^{(m)} +f_i^{(m)}w_i^{(m)}+\frac{1}{\rho\cdot A}\cdot\exp\left(\frac{\|v_R^{(m)}\|}{v_a}\cdot\rho\right)\right)+\Lambda\right\}\cdot\boldsymbol{n}$$
$$\text{on } \Gamma_{design}\equiv\Gamma\backslash\Gamma_{fix} \qquad (28)$$

So long as the shape gradient function can be derived theoretically, domain variation can be analyzed by the traction method.

3. Numerical Solution Technique

3.1 Traction method

The traction method is a procedure for finding the amount of domain variation (speed field $\boldsymbol{V}$) that reduces the objective functional, based on governing Eq.(29). This method uses the gradient method in a Hilbert space, a technique that is also employed in distributed parameter optimal control problems.

$$a(\boldsymbol{V},\boldsymbol{w})=-l_G(\boldsymbol{w}) \quad \text{for all } \boldsymbol{w}\in\boldsymbol{C}_\Theta \qquad (29)$$

Governing Eq.(29) indicates that the speed field $\boldsymbol{V}$ is found as a displacement field when the negative shape gradient function $-\boldsymbol{G}$ acts on the boundary or the domain as an external force. In other words, with the traction method the domain variation is found as a displacement field when the shape gradient function acts as an external force in a pseudo-elastic problem. Accordingly, Eq.(29) can be solved with a solution to ordinary linear-elastic problems, confirming the general applicability of the traction method. In this paper, the finite element method is used. Moreover, the traction method also offers the advantages that there is no need to refine the mesh and that boundary smoothness is assured following domain variation[10].

With the aim of applying the traction method to a wide range of practical design problems, the authors have developed a shape optimization system that uses a general-purpose FEM code. This general-purpose code, I-DEAS, has also been used in this work as a

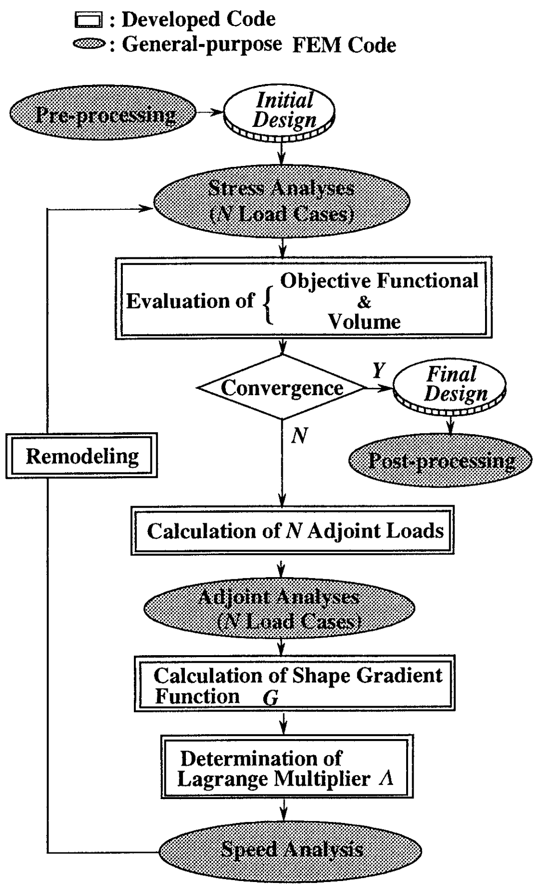

Fig. 3 Schematic flow chart of shape optimization system

type of subroutine to solve Eqs.(16),(17) and (29). A flow chart of the shape optimization system is shown in Fig. 3. The objective functional is minimized and the optimum shape is obtained by repeating the stress analysis (Eq.(16)) to evaluate the objective functional and to find the shape gradient function, the adjoint analysis (Eqs.(17) or (26)), the speed analysis to determine the speed field $\boldsymbol{V}$ (Eq. 29), and updating the shape. The boundary conditions (side constraint and adjoint load) set for domain variation in the speed analysis are independent of and different from the boundary conditions defined in the stress analysis.

3.2 Calculation of adjoint variables

This section explains the specific procedure for solving adjoint Eqs.(17) and (26) that are characteristic of the problems treated here.

Adjoint Eq.(17) can be expressed in the following matrix notation:

$$\int_{\Omega_S}[B^{(m)}]^T[D][B^{(m)}]dx\{w^{(m)}\}$$
$$=\int_{\Omega_S}[B^{(m)}]^T[D]\left\{\frac{1}{\sigma_a A}\exp\left(\frac{\sigma_M^{(m)}}{\sigma_a}\cdot\rho\right)\cdot\frac{\partial\sigma_M^{(m)}}{\partial\sigma_{ij}}\right\}dx \tag{30}$$

where $[B]^T$ indicates the transposed matrix of the strain-displacement matrix $[B]$ and $[D]$ indicates the elastic matrix. By applying the distributed initial strain in the domain

$$\left\{\frac{1}{\sigma_a A}\exp\left(\frac{\sigma_M^{(m)}}{\sigma_a}\cdot\rho\right)\frac{\partial\sigma_M^{(m)}}{\partial\sigma_{ij}}\right\}$$

as an external force, the adjoint displacement $\boldsymbol{w}$ is found. The initial strain can also be converted to a thermal strain and applied in that form(7). Further, in the case of adjoint Eq.(26), the adjoint displacement $\boldsymbol{w}$ is found by giving the distributed load in the domain

$$\left\{\frac{1}{v_a A}\cdot\exp\left(\frac{\|v_k^{(m)}\|}{v_a}\cdot\rho\right)\cdot\frac{\partial\|v_k^{(m)}\|}{\partial v_k}\right\}$$

as an external force.

3.3 Consideration of constraints

Two procedures for considering constraints have been used so far in applying the traction method to actual design problems. One procedure, based on the concept of PID (proportional-integral-derivative) control, is effective in treating a single equality constraint(11). The other procedure can also treat multiple constraints(12). In this paper, the procedure based on the concept of PID control is used. Specifically, the Lagrangian multiplier Λ, which is determined so as to satisfy the volume constraint, can be regarded as a uniform surface traction within the force $-\boldsymbol{G}$. The volume constraint is then satisfied by controlling the magnitude of the uniform surface traction Λ.

4. Computed Results

The shape optimization system was applied to min-max stress and displacement problems in order to verify the effectiveness and practical utility of the proposed method. The min-max stress problems were fundamental two-dimensional problems involving a fillet and a torsion arm and a three-dimensional problem involving a solid arm. The min-max displacement problems involved a two-dimensional bent plate, a fillet and a torsion arm. The latter two problems were similar to the min-max stress problems and were considered for the sake of comparing the optimal shapes. In all of the problems, the initial volume (area) was given as a constraint. The maximum value of the initial shape in each problem was used as the normalization constant σ_a or v_a. The two-dimensional problems assumed a condition of plane stress, and four node elements were used in the numerical analysis. The value of ρ in the KS function was set at 30.

4.1 Min-max stress problems

4.1.1 2D single-loading fillet problem The problem statement of a fillet design in which the objective was to minimize the maximum stress is shown in Fig. 4. In the stress analysis, one end of the part was subjected to a sliding constraint and a distributed load P was applied to the other end, as shown in Fig. 4(a). In the speed analysis, only the fillet portion was specified as the design boundary and the remaining boundaries were treated as being invariable. The analysis was performed with a symmetrical half model.

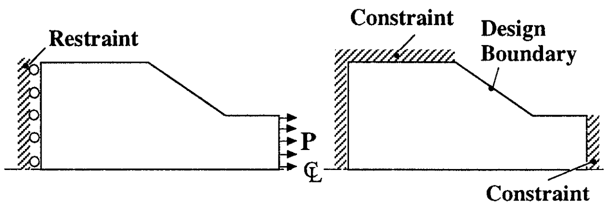

(a) Stress analysis (b) Speed analysis

Fig. 4 Fillet Problem

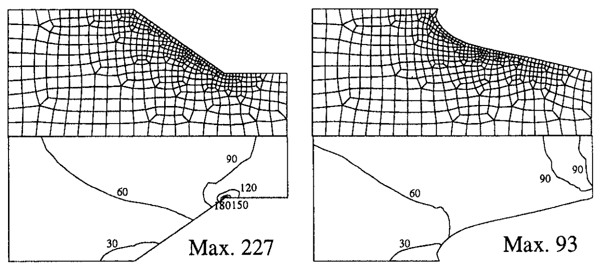

Fig. 5 Initial and optimal shapes and stress distributions [MPa]

The initial shape and optimal shape obtained are shown in Fig. 5 along with their von Mises stress distributions. Iteration histories normalized to the value of the initial shape are given in Fig. 6. The maximum stress was reduced by approximately 60%, and the fillet portion shows a uniform stress distribution, except in the vicinity of the fixed boundaries. The results confirm that the objective functional and the maximum stress were minimized.

4.1.2 3D single-loading solid arm problem The min-max stress problem statement for a solid arm subject to compressive loading is shown in Fig. 7 as an example of an application to a three-dimensional problem. As the boundary conditions in the stress analysis, the circumference of a circular hole was fixed and a distributed compressive load P was applied to the other end, as shown in Fig. 7(a). The constraints applied in the speed analysis consisted of constraints that allowed domain variation along its width and thickness, as indicated in Fig. 7(b). A solid element with eight nodes was used in the numerical analysis which was performed with a symmetrical half model.

The initial shape and the optimal shape obtained are shown in Fig. 8 along with their von Mises stress distributions. Iteration histories normalized to the initial values are given in Fig. 9. The maximum stress was reduced by approximately 30% and a uniform stress distribution was obtained over nearly the entire arm, except for a portion around the circumference of the hole. Similar to the results of the two-dimensional problem, the objective functional and the maximum stress were minimized. These results confirm that the proposed method can also be used to find optimal shapes in three-dimensional problems.

4.1.3 2D multiple-loading torsion arm problem The min-max stress problem statement for a torsion arm subject to multiple loading is shown in Fig. 10. As shown in Fig. 10(a), the circumference of a circular

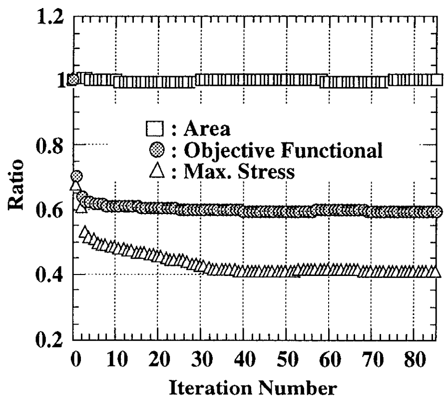

Fig. 6 Iteration histories

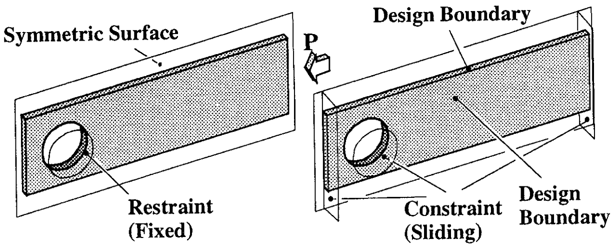

(a) Stress analysis (b) Speed analysis

Fig. 7 Solid arm problem

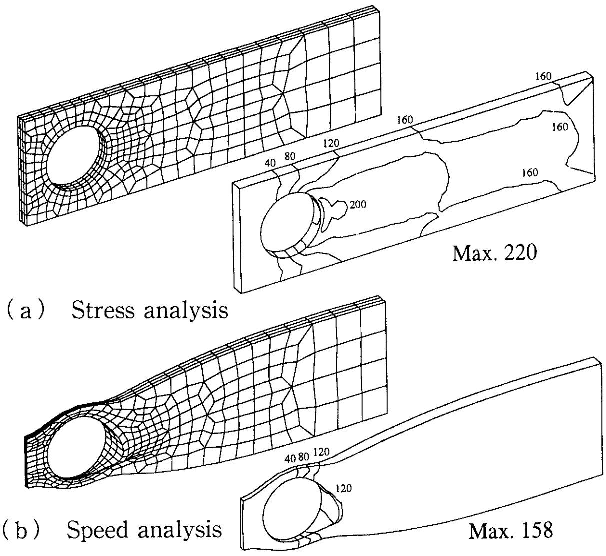

Fig. 8 Initial and optimal shapes and stress distributions [MPa]

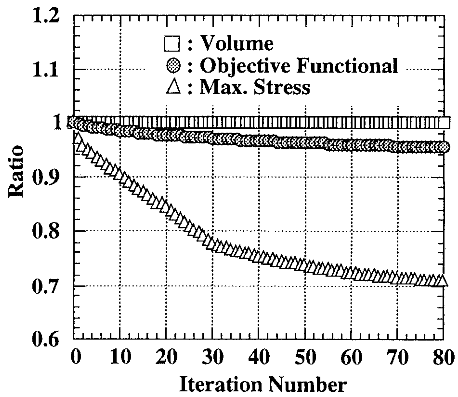

Fig. 9 Iteration histories

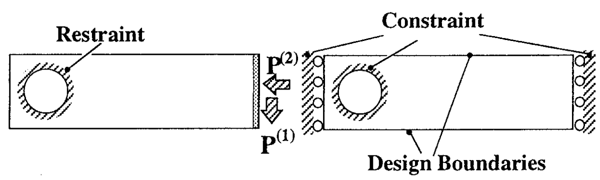

(a) Stress analysis (b) Speed analysis

Fig. 10 Torsion arm problem

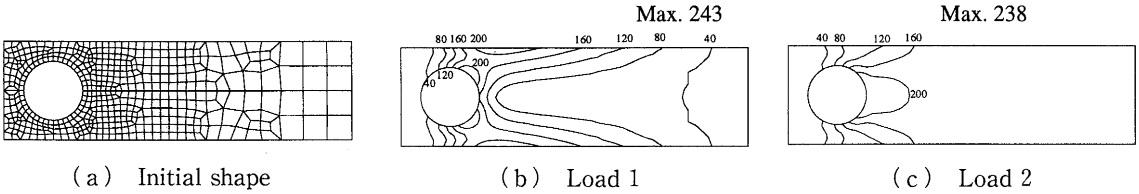

Fig. 11 Initial shape and stress distributions for multiple loads [MPa]

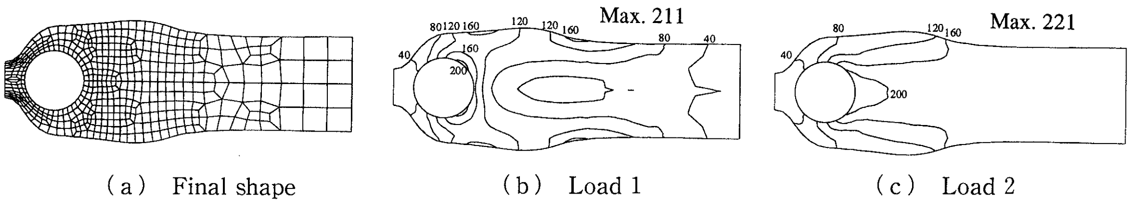

Fig. 12 Optimal shape and stress distributions for multiple loads [MPa]

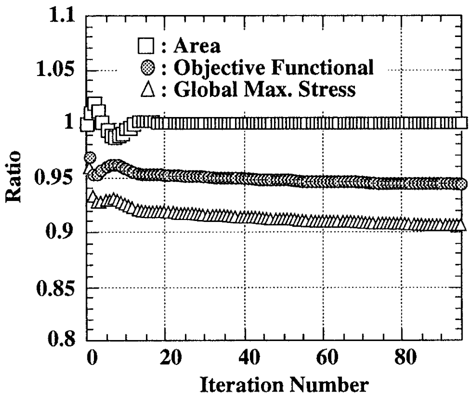

Fig. 13 Iteration histories (load 1 and load 2)

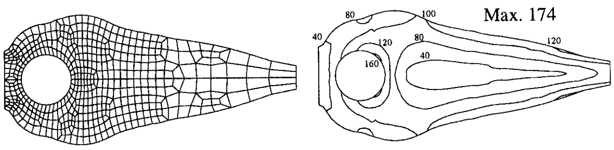

Fig. 14 Optimal shape and stress distribution for load 1 [MPa]

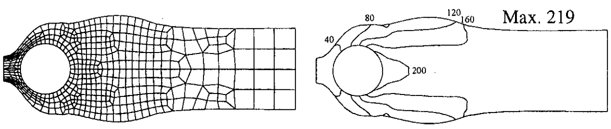

Fig. 15 Optimal shape and stress distribution for load 2 [MPa]

hole was fixed in the stress analysis and two types of distributed loads, $P^{(1)}$ and $P^{(2)}$, were applied to the other end. In the speed analysis, a fixed constraint was applied to the circumference of the hole and sliding constraints were applied to both ends of the arm, as indicated in Fig. 10(b).

Figures 11 and 12 show the initial shape and optimal shape obtained along with the von Mises stress distributions for the two load cases. Iteration

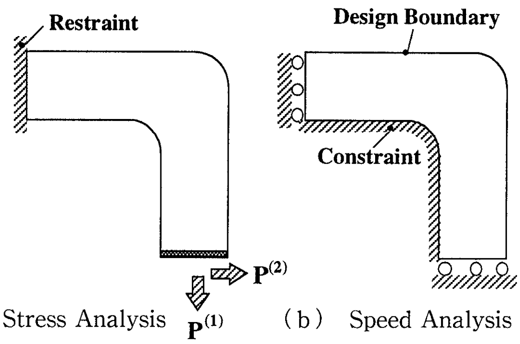

Fig. 16 Bent plate problem

histories normalized to the value of the initial shape are given in Fig. 13. The results indicate that the objective functional and maximum stress were minimized, verifying that the proposed method also functioned effectively in this multiple-loading problem. For the sake of comparison, the optimal torsion arm shape calculated for each load individually is shown in Figs. 14 and 15.

4.2 Min-max displacement problems

4.2.1 2D multiple-loading bent plate The problem statement for a bent plate is shown in Fig. 16 as an example of a min-max displacement problem. As shown in Fig. 16(a), one end of the plate was fixed in the stress analysis and two types of distributed loads, $P^{(1)}$ and $P^{(2)}$, were applied to the other end. In the speed analysis, the outer shape was specified as the design boundary, as indicated in Fig. 16(b).

Figure 17 shows the initial shape and optimal shape obtained along with the deformation modes for the two load cases. Iteration histories normalized to the value of the initial shape are given in Fig. 18. Both the objective functional and the maximum displacement were minimized, confirming that the proposed method is also applicable to min-max displacement problems.

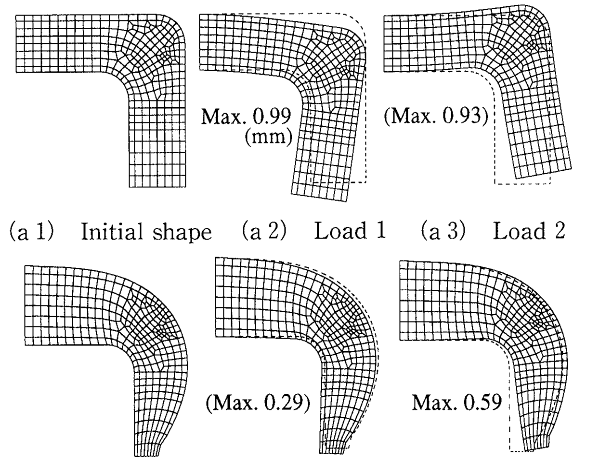

(a 1) Initial shape (a 2) Load 1 (a 3) Load 2

(b 1) Final shape (b 2) Load 1 (b 3) Load 2

Fig. 17 Initial and optimal shapes and deformation modes

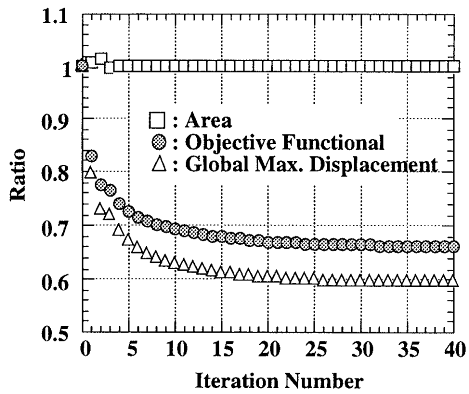

Fig. 18 Iteration histories

4. 2. 2 2D single-loading fillet problem Calculations were performed for a min-max displacement problem involving a fillet subject to the same conditions as in section 4. 1. 1. The optimal shape obtained is shown in Fig. 19. The shape resembles that obtained in the min-max stress problem (Fig. 5), although slight differences are observed near the loading point owing to the influence of the adjoint load.

4. 2. 3 2D single-loading torsion arm problem Min-max displacement calculations were performed for the torsion arm when it was subjected only to the $P^{(1)}$ load case mentioned in section 4. 1. 3. Figure 20 shows the optimal shape obtained. The maximum displacement was reduced by 34%. A comparison with the shape obtained in the min-max stress problem (Fig. 14) reveals that the optimum stress is approximately 13% higher and that the shape is also clearly different.

These results indicate that the optimal shapes for min-max displacement and min-max stress problems do not always coincide. This discrepancy is attributed to differences in the strain fields of the adjoint analyses.

5. Conclusion

This paper has presented a numerical method for solving boundary shape optimization problems in which the objective is to minimize some maximum local measure under multiple loading conditions. The local measures considered here were von Mises stress and the displacement norm. The specific procedure of

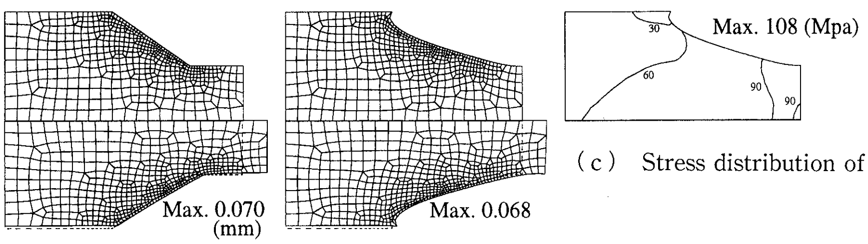

(c) Stress distribution of final shape

(a) Initial shape (b) Final shape

Fig. 19 Initial and optimal shapes

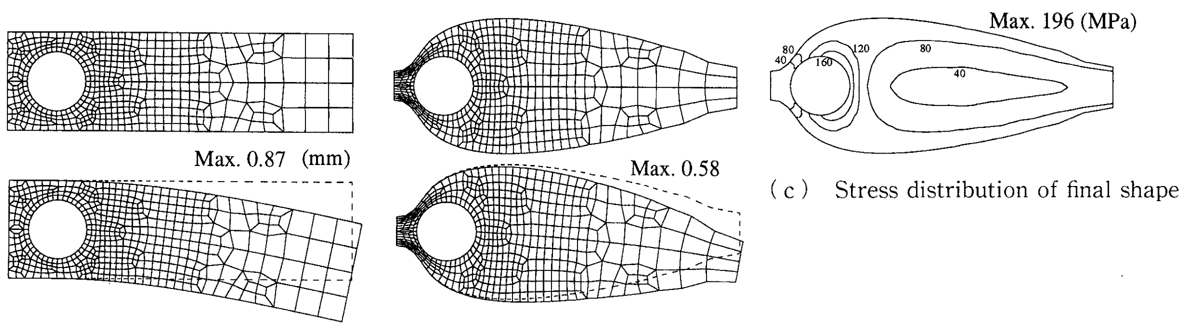

(c) Stress distribution of final shape

(a) Initial shape (b) Final shape

Fig. 20 Initial and optimal shapes

the proposed method is as follows.

(1) Using the *KS* function, a multiple loading problem is simplified and formulated as a solvable single-objective problem.

(2) The shape gradient function of the recast problem is derived theoretically using the material derivative method and the adjoint variable method.

(3) By applying the shape gradient function with the traction method, the amount of domain variation that minimizes the objective functional is found numerically.

Calculated results for typical two- and three-dimensional problems were presented to demonstrate the effectiveness of the proposed method. This method makes it possible to obtain optimal shape designs that minimize the maximum stress or maximum displacement of the structure.

References

(1) Banichuk, N.V., Introduction to Optimization of Structures, (1990) p. 32-35, Springer-Verlag, New York.

(2) Taylor, J.E. and Bendsøe, M.P., An Interpretation for Min-Max Structural Design Problems Including a Method for Relaxing Constraints, Int. J. Solids Struct., Vol. 20, No. 4 (1984), p. 301-314.

(3) Trompette, P. and Marcelin, J.L., On the Choice of Objectives in Shape Optimization, Eng. Opt., Vol. 11 (1987), p. 89-102.

(4) Kristensen, E.S. and Madsen, N.F., On the Optimum Shape of Fillets in Plates Subjected to Multiple In-plane Loading Cases, Int. J. Num. Meth. Eng., Vol. 10 (1976), p. 1007-1019.

(5) Azegami, H., Trans. Jpn. Soc. Mech. Eng., Vol. 60, No. 574, A (1994), p. 165 (in Japanese).

(6) Shimoda, M., Azegami, H. and Sakurai, T., Trans. Jpn. Soc. Mech. Eng., Vol. 62, No. 602, A (1996), p. 2393-2400 (in Japanese).

(7) Shimoda, M., Azegami, H. and Sakurai, T., Trans. Jpn. Soc. Mech. Engs., Vol. 62, No. 604, A (1996), p. 2831-2837 (in Japanese).

(8) Kreisselmeier, G. and Steinhauser, R., Systematic Control Design by Optimizing a Vector Performance Index, International Federation of Active Control Symposium on Computer-Aided Design of Control Systems, (1979-8), Zurich, Switzerland, p. 113-117.

(9) Wrenn, G.A., An Indirect Method for Numerical Optimization Using the Kreisselmeier-Steinhauser Function, NASA Contractor Report 4220 (1989).

(10) Azegami, H., Kaizu, S., Shimoda, M. and Katamine, E., Proc. of the First Con. on Comp. Eng. and Science, Vol. 1 (May 1996), p. 625-628.

(11) Shimoda, M., Azegami, H. and Sakurai, T., JSME Int. J., Ser. A, Vol. 39, No. 3 (1996), p. 407-414.

(12) Shimoda, M., Sakurai, T., and Azegami, H., Shape Optimization of Linear Elastic Structures Subject to Multiple Loading Conditions - A Traction Method Approach to Minimum Volume Design - in Current Topics in Computational Mechanics, J. F. Cory, Jr. and J. L. Gordon (Eds.), PVP-Vol. 305 (1995), p. 319-326, ASME.